Variable-source flood pulsing in a semi-arid transboundary watershed: the Chobe River, Botswana and Namibia

Narcisa G. Pricope

Abstract The Chobe River, characterized by an unusual flood pulsing regime and shared between Botswana and Namibia, lies at the heart of the world's largest transfrontier conservation area (the Kavango–Zambezi Transfrontier Conservation Area). Significant ecological changes and vegetation conversions are occurring along its floodplains. Various scenarios for agricultural and urban water use are currently being proposed by the government of Botswana. However, the understanding of the river's annual flow regime and timing of the relative contributions of water from three different sources is relatively poor. In light of past and future climate change and variability, this means that allocating water between ecological flows and economic and domestic uses will become increasingly challenging. We reconstruct the inundation history in this basin to help ease this challenge. This paper presents a spatiotemporal approach to estimate the contribution of water from various sources and the magnitude of changes in the flooding extent in the basin between 1985 and 2010. We used time series analysis of bimonthly NOAA AVHRR and NASA MODIS data and climatologic and hydrologic records to determine the flooding timing and extent. The results indicate that between 12 and 62 % of the basin is flooded on an annual basis and that the spatial extent of the flooding varies throughout the year as a function of the timing of peak discharge in two larger basins. A 30-year trend analysis indicates a consistent decline in the average monthly flooded area in the basin. The results may prove useful in future water utilization feasibility studies, in determining measures for protecting ecological flows and levels, and in ecosystem dynamics studies in the context of current and future climate change and variability.

Introduction

Wetlands and seasonally inundated floodplains in semi-arid environments play major roles in the regional and global biogeochemical cycling of methane and carbon dioxide, habitat diversity, hydrologic cycles, and their influence on human disease and livelihood support systems through controls on fisheries productivity, water availability, and flood recession agriculture (Prigent et al. 2007; Appleton et al. 2008). Wetlands and seasonally inundated systems have historically been recharged during regular flooding events, but their hydrology has been altered to various

N. G. Pricope (✉)
Environmental Studies Department,
Southern Oregon University,
1250 Siskiyou Blvd,
Ashland, OR 97520, USA
e-mail: pricopen@sou.edu

degrees by climatic variability and shifts in large-scale atmospheric circulation patterns, human control over natural rivers, or increasing demand for growing population centers (Jia and Luo 2009). In semi-arid regions in particular, flooding regimes are increasingly influenced by climate change and variability, water regulations and water shortages, and increasing water demands from agricultural, industrial, and domestic uses. In water-scarce regions, analyses of the spatial extent and temporal pattern of flooding are important for understanding ecosystem processes and changes. Also, understanding past spatiotemporal changes in flooding regimes is critical in water resource management and for flood prediction and mitigation measures. However, long-term flood inundation mapping in these regions is difficult due to the lack of historical flow data and of spatially distributed ground data. Therefore, repetitive, synoptic, remotely sensed data (usually of moderate or coarse resolution) can be used to reconstruct the flooding regime. Understanding how the flooding regime in a semi-arid watershed adapted to seasonal flood pulses has changed through time can then enable us to understand the links with ecosystem-level changes. It can also prove useful in making more informed management decisions to optimize the allocation of a scarce resource among relatively conflicting uses.

While the interaction between precipitation, drought, fire, and grazing on arid environments has been the subject of considerable research, less is known about the impact of flooding, or the lack of flooding in flood-adapted ecosystems, and how flooding interacts with other factors in modifying vegetation structure and driving landscape dynamics (Westbrooke and Florentine 2005). Westbrooke et al. (2005) have shown that flooding was the most important factor for determining changes in vegetation composition in an arid basin in Australia, while fire and grazing were of much less importance·, as water availability directly affects rooting depth for grasses vs. shrubs. Ringrose et al. (2007) concluded that water table lowering, driven by localized desiccation and resulting in increased soil salinization, led to compositional and functional changes in trees and shrubs in the semi-distal areas of the Okavango Delta in Botswana. More specifically, the lowering of the water table below the effective root depth of trees and increasing salinization led to invasions by relatively shallower-rooted woody vegetation, which is more

brackish water-tolerant. Westbrooke and Florentine (2005) also showed that perennial grass and perennial shrubs are the most likely to be influenced by rare flooding events, which means that water availability is a significant control factor in grassland-to-scrub transitions. This is because, as the surface layers become drier, the density of shrubs increases and species are selected based on their ability to access water in deeper layers of the soil horizon.

Variations in water availability at different temporal and spatial scales in semi-arid ecosystems in terms of mean annual precipitation (MAP) variability, length of growing season, period between precipitation events, and number of precipitation events during the wet season are the most important drivers of ecosystem change (Snyder and Tartowski 2006; Peters and Havstad 2006). For flood-dependent ecosystems, soil moisture availability and extent of flooding are also important drivers of change in vegetation (Boulain et al. 2006). In semi-arid savannas characterized by a MAP value <650 mm, trees and grasses coexist as a result of water limitations on woody cover. While disturbances (fire and grazing) are able to modify tree/grass ratios, they are not required for the coexistence of trees and grasses, as opposed to savannas with an MAP >650 mm where disturbances are needed for coexistence (Sankaran et al. 2005). This might mean that future changes in precipitation and in the flooding patterns for the flood-adapted ecosystems can have effects on savanna dynamics and, depending on the temporal scale of change, determine the nature of interaction between precipitation and disturbances.

To understand the dynamics of flood pulsing and the potential implications for ecosystem change, we need to consider the relationship between climate variability, long-term river runoff variations, and flooding dynamics through time. While climate change forecasts are mixed for the Southern African region, some indicate a potential reduction in river runoff associated with changing patterns of precipitation and increasing temperatures (Boko et al. 2007). This might mean that allocating water between ecological flows and economic and domestic uses will become increasingly challenging, especially for watersheds with limited historical flow data. Such a watershed is where we focused our analysis. The Chobe system, hereafter referred to as the Chobe River Basin (CRB), is a waterway shared between Namibia and Botswana, situated at the heart of

one of Southern Africa's largest transfrontier conservation areas: the Kavango–Zambezi (KAZA) Transfrontier Conservation Area. KAZA is an ongoing joint multilateral effort among several Southern African countries toward resource co-management and wildlife habitat conservation. Understanding the inundation dynamics in this basin is also important for habitat and wildlife conservation efforts given the preeminence of wildlife-based tourism accounting for large portions of the gross domestic product in both countries.

Climatically, Nicholson et al. (2000) have shown that, while before the 1960s rainfall was above the long-term mean in much of Africa, Southern Africa experienced negative anomalies in the order of 10–20 %. These rainfall deficits continued through the 1970s and 1980s, and well into the 1990s when rainfall in Southern Africa remained below the long-term mean (Nicholson et al. 2000, 2001). Work by Wessels et al. (2004) in South Africa indicated that rainfall for the late 1980s was below the 50-year average, while oscillations between wet and dry years starting with the early 1990s have become more extreme under the influence of stronger El Niño or La Niña years. They also found that for Southern Africa, 1991–1992, 1994–1995, and 1997–1998 have been the driest El Niño seasons while 1999–2000 and 1995–1996 the wettest seasons, with the 2001–2002 and 2003–2004 growth seasons being the driest. Studies which link long-term climate variability to river runoffs and seasonal inundation extents for this region of Africa have been scarce, and we include analyses of long-term discharge and precipitation data to understand what the overall trends in these data have been for the last three decades.

Monitoring surface water resources using satellite imagery is an increasingly important tool for the prediction of floods and droughts (Alsdorf and Lettenmaier 2003). For instance, Landsat imagery has been used extensively to measure areas inundated by flood waters (Smith 1997; Domenikiotis et al. 2003; McCarthy et al. 2003). Advanced Very High Resolution Radiometer (AVHRR) and Moderate-Resolution Imaging Spectroradiometer (MODIS) time series vegetation indices data were used successfully in previous studies for mapping flooding and the extents of inundation (Bryant 1999, 2003; All and Yool 2004; Brown et al. 2006; Chipman and Lillesand 2007; Sakamoto et al. 2007; Wang and D'Sa 2010). The delineation of flooded areas using vegetation indices as a proxy for the amount of green

vegetation depends on the type of vegetation, canopy cover percentages, soil type, the time interval after the event, and the spatial extent of the area affected (Domenikiotis et al. 2003). Vegetation indices represent a continuous variable related to the productivity of land cover or vegetation biomass, which varies both in space and time, and have a very distinct spectral signature for water, as opposed to land (Domenikiotis et al. 2003). Of the multitude of multispectral vegetation remote sensing-based indices that have been developed, the Normalized Difference Vegetation Index (NDVI) is the most widely used (Teillet et al. 1997); however, it is sensitive to atmospheric aerosols and soil background.

Others working in estuarine wetlands have found the Enhanced Vegetation Index (EVI) to be more suitable because it provides better results than the NDVI when the humidity and soil moisture are high (Sakamoto et al. 2007). EVI is calculated using the red, near-infrared, and blue reflectance values of MODIS bands 1, 2, and 3, respectively, and uses a gain factor and a canopy background adjustment factor, as well as two coefficients of aerosol resistance that employ the blue band to correct aerosol influences in the red band (Liu and Huete 1995; Yan et al. 2010). The EVI is more sensitive in dense vegetation types such as forests and agricultural areas and usually reduces the noise effects of canopy background and atmospheric aerosols (Justice et al. 1998). Sakamoto et al. 2007 employed the MODIS EVI product to determine temporal changes in the annual flooding extent in the Mekong Delta and have shown that the spatial extent of flooding determined from the satellite data is in excellent agreement with the water-level data recorded at hydrologic stations on the ground. The main drawback to such datasets (AVHRR and MODIS), however, is their low spatial resolution, but their high temporal frequency of global coverage, high repetitiveness, wide swath, and low cost compensate for the low spatial resolution (McCarthy et al. 2003; Jain et al. 2006).

The Chobe River is, in most stream classification systems in the region, considered a tributary of the Zambezi River. However, in reality, it has a most unusual flow regime consisting of variable flood pulses arriving at different times of the year from rivers with headwaters in the tropical regions of Angola and Zambia, such as the Kwando and Zambezi Rivers. Little is understood in this system about the spatial and temporal dynamics of inundation as it has never been studied from this perspective before. This paper addresses two interrelated research questions:

1. What is the intra-annual timing and spatial distribution of inundation in the CRB relative to the distribution of regional precipitation and discharge in the two main contributing rivers (the Zambezi and Kwando Rivers)?
2. Has the spatial extent of flooding changed in the CRB over the last 30 years?

We hypothesized that there has been a decrease in the spatial flooding extent and, more generally, a change in the timing and frequency of flooding in the CRB system in the last 30 years, assuming that the decreasing rainfall patterns described by Nicholson (2000) apply for the CRB and further supported by key informant interviews. This hypothesis was tested using remote sensing techniques to determine flooded vs. non-flooded areas and hydrologic and climatologic records to compare to the time series remote sensing analysis. If this hypothesis was supported, we expected the time series analysis using bimonthly 1985–2000 AVHRR and 2000–2010 MODIS vegetation indices data to indicate a bimonthly and seasonal reduction in the extent of flooding, expressed in the ratio of water to land pixels in every image for the basin. However, this hypothesis was slightly complicated by the fact that recent years starting in 2008 have shown a general trend of above normal precipitation for this region; this will be discussed in the second part of this paper.

The specific research objectives addressed in this paper are:

(a) To map the intra-annual spatial distribution of the flood pulse in the CRB relative to runoff in the Zambezi and Kwando Rivers and regional precipitation
(b) To reconstitute the inter-annual distribution of the flood pulse in CRB and create a flooding extent index (focusing primarily on the higher-resolution MODIS time series data, available for 2000 to 2010)
(c) To conduct a longitudinal (time series) analysis of changes in the spatial extent of flooding in CRB

Data and methods

Study area

The CRB has a mosaic of land use and management units: subsistence communal lands predominantly utilized for livestock grazing or agricultural lands; differently managed forest reserves in both countries; a national park (Chobe National Park); and an urbanizing area, the town of Kasane. CRB was divided into three distinct subsystems for this analysis to address the interconnectedness question: Mamili wetland, the Chobe–Linyanti system, and Zambezi wetlands (Fig. 1). Visible ecological and vegetation changes have occurred in this region in the last 30 years, possibly caused by increases in wildlife populations, decreases in rainfall and river inundation extent, and increasing population and utilization by cattle (Mosugelo et al. 2002; Skarpe et al. 2004; Rutina et al. 2005).

The Chobe receives water through surficial and underground connections from several sources. The most important source in terms of the amount of water is the Zambezi River which pushes various amounts of water back into the Chobe, depending on its discharge and to a smaller degree on regional precipitation. During a secondary flood pulse fed by flood waters from the Kwando River through the Mamili wetlands, CRB receives water through sporadic connections from Lake Liambezi and the Linyanti channel. This dry season flood pulse occurs because the Kwando River discharge peaks in June–July, as opposed to March–April, as is the case for the Zambezi River (Fig. 2). Once the peak discharge in the main trunk of the Zambezi begins to recede, and depending also on the amount of water being pushed forward from the Kwando through the Linyanti channel and Lake Liambezi into CRB, the Chobe then flows forward into the Zambezi, becoming a tributary. Other sources of water inflow into CRB are represented by surface and groundwater connections with the Zambezi River across the Caprivi Region through the Zambezi wetlands and by variable contributions from local and regional precipitation, primarily during the wettest months from December to February (Fig. 3). Very infrequently and only during years of high flooding such as 2009 and 2010, the CRB receives small amounts of inflow from the Kavango River and Okavango Delta through an ephemeral channel called the Selinda Spillway. This unusual flow regime, which has never before been studied in detail, is mainly the result of geotectonic modifications through time and is currently reinforced by the presence of relatively active fault lines in the region, such as the Linyanti Fault, which is the main geologic control for the present-day location of the Chobe–Linyanti channel (Gumbricht et al. 2001).
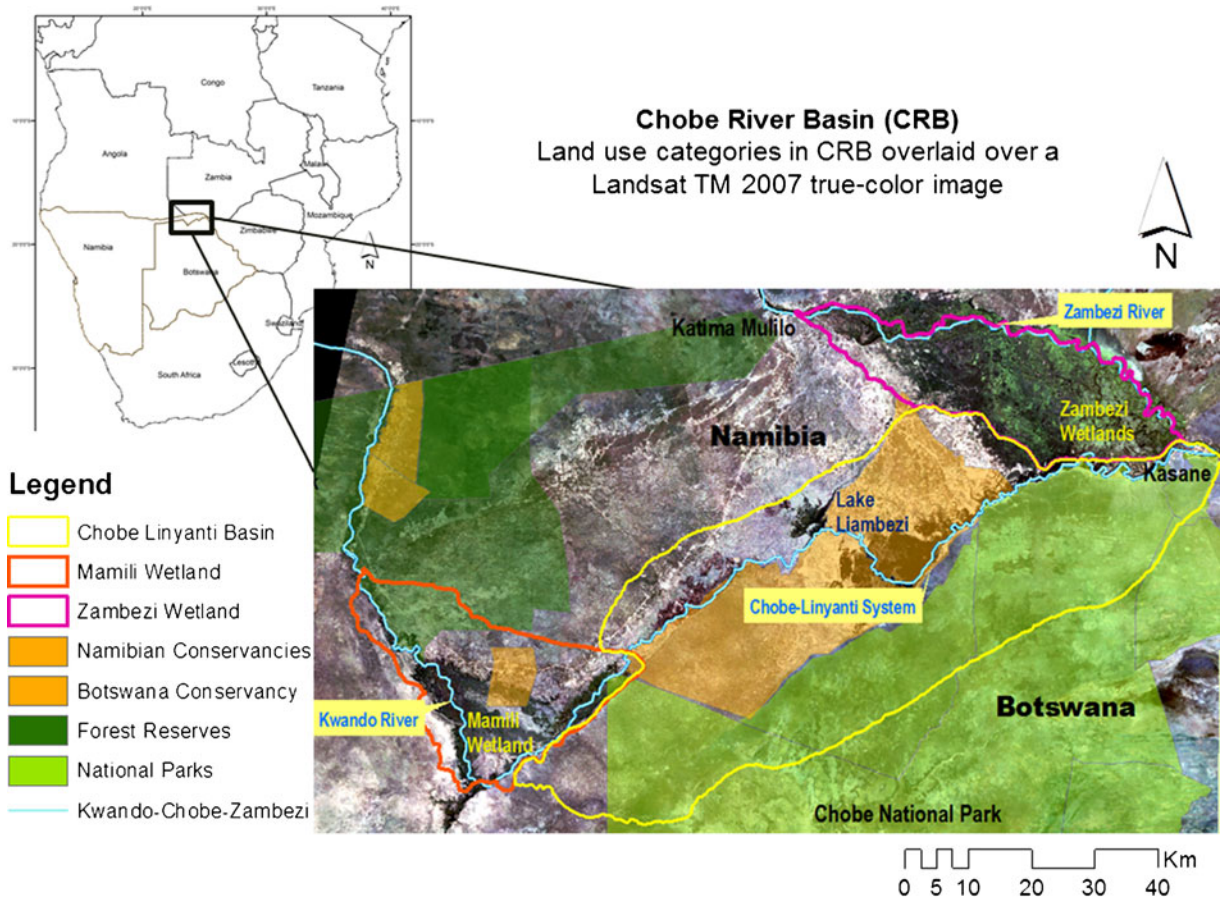
Fig. 1 Study area showing the CRB in Southern Africa and the main land management categories in the basin. Also shown are the three interlinked river systems: the Kwando River and the Mamili wetland to the southwest, the Linyanti and Chobe system, and the Zambezi River and Zambezi wetlands to the northeast. The national boundary between Namibia and Botswana follows the Chobe–Linyanti River

The contributions and timing of inflow into CRB from these different sources are variable in both time and space and have never been studied in any detail; therefore, the understanding of the annual flow and flood pulsing regime of the Chobe system is relatively poor. The annual flood pulse in the Chobe River is one of the major factors characterizing the regional ecosystem and human activities in the region. The Chobe River is economically and ecologically important to both Namibia and Botswana and is especially important for the KAZA Region as it provides critical habitat for various migratory wildlife populations, in particular the largest elephant population in Africa—over 200,000 elephants (DWNP 2009)—centered around Chobe National Park. Given the fact that 94 % of Botswana's water resources have their headwaters in other Southern African countries (Turton

1999), and that the flow of the Chobe River is largely regulated by back-flooding from the Zambezi River and seasonal contributions from the Kwando River to the northwest, establishing the flooding regime of the Chobe River for the last 30 years is of significance to water resource and land resource managers, especially given new developments in irrigated agriculture proposed by Botswana and the crucial importance of this water source to both wildlife and human populations in both riverine countries.

Data sources

We used a combination of varying spatial and temporal resolutions remotely sensed datasets, such as AVHRR, MODIS, and Landsat ETM+; ground data from several field seasons in the region; and ground
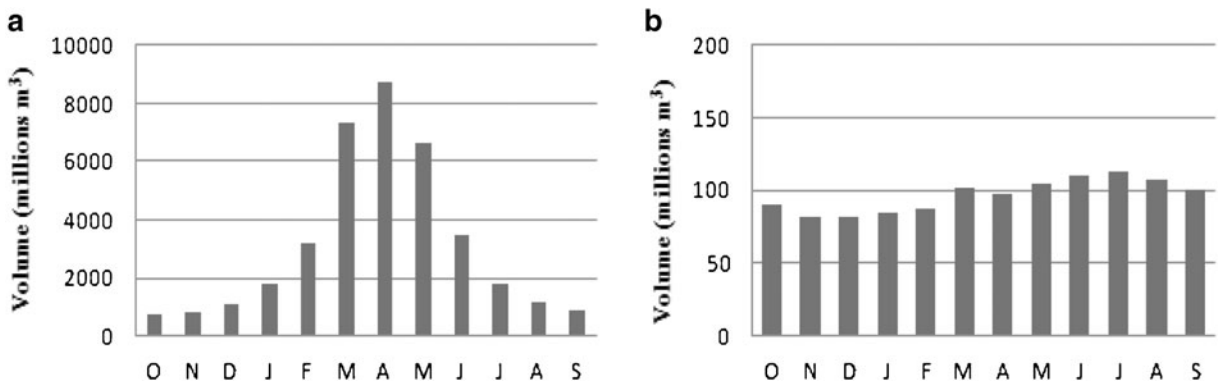
Fig. 2 Long-term average monthly discharge of the Zambezi (a) and Kwando (b) Rivers for the period 1965–2009 plotted from the beginning of the hydrologic year—October to September (data source: Department of Water Affairs, Namibia). Such a hydrograph is not available for the Chobe River

and satellite climatologic and hydrologic datasets to understand the timing and dynamics of flooding in the Chobe River Basin (Table 1).

AVHRR and MODIS time series vegetation indices

A continuous series of 623 AVHRR high-resolution picture transmission (HRTP) images were acquired in atmospherically and spectrally calibrated maximum value composite (MVC) 10-day NDVI form from the archive of the Coarse Resolution Imagery Database (CRID) of the Institute for Soil, Climate and Water,

Agricultural Research Council of South Africa. AVHRR vegetation indices, particularly NDVI, data have been used successfully in previous studies to determine the extent of inundation at various geographic scales (Birkett 2000; Prigent et al. 2007).

The first MODIS image available for the region is for February 2000. The MODIS Vegetation Indices (VI) 250-m spatial resolution data (MOD13Q1A) were acquired from USGS's Land Processes Distributed Active Archive Center (LP DAAC) and re-projected to the Universal Transverse Mercator, the WGS84 coordinate system using nearest neighbor
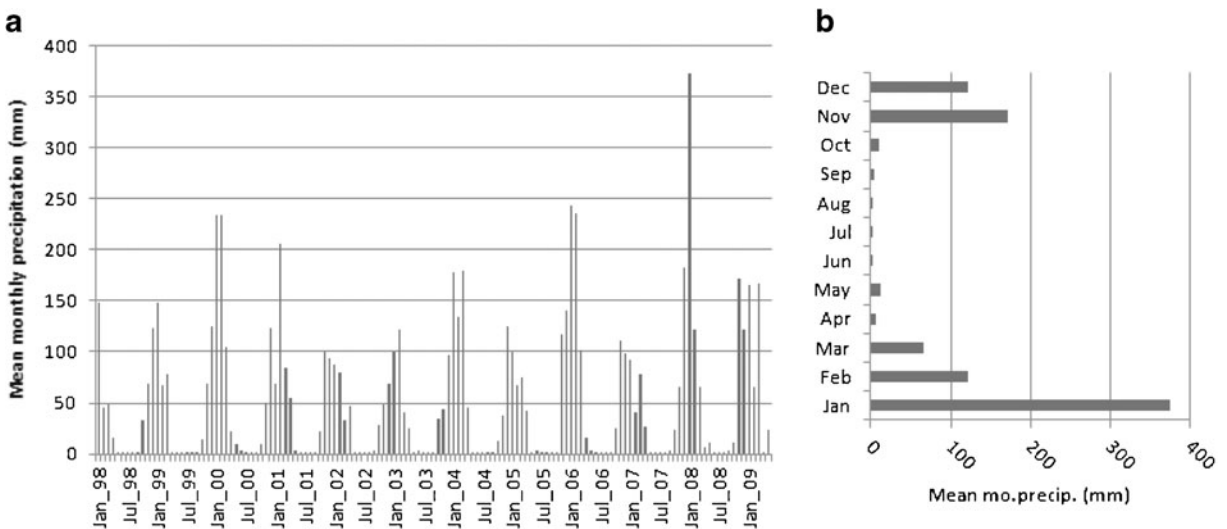

Fig. 3 a Mean monthly rainfall data from the Tropical Rainfall Measuring Mission (TRMM 3B43) for the period January 1998 to May 2009 for the Chobe River Basin. b Mean monthly rainfall for 2008 in CRB showing the intra-annual typical distribution of precipitation (in millimeters)

Table 1 Data types, temporal and spatial resolutions, sources of data, and their temporal availability

Data categories	Data type	Data source	Temporal availability
Remotely sensed	AVHRR NDVI 10-day MVC 1.1-km^2 data	Coarse Resolution Imagery Database (CRID), South Africa	September 1985–April 2000
Data	(AVHRR HRTP) MODIS EVI 16-day 250-m^2 data (MOD 13QA)	USGS Land Processes Distributed Active Archive Center (LP DAAC)	April 2000–April 2010
	Landsat ETM+ 30-m^2 multispectral data	USGS Earth Explorer, University of Maryland Global Land Cover Facility, Council for Scientific and Industrial Research, South Africa	April/May 1986, 1990, 1996, 2002, 2003, 2004, 2007, 2009
Climatologic data	Multivariate ENSO Index (MEI)	National Oceanic and Atmospheric Administration	1950–2010
	Station rainfall data	Department of Meteorological Services Botswana	1945–2008
	Tropical Rainfall Measuring Mission (TRMM 3B43) rainfall data	NASA's Goddard Space Center	1998–2009
Hydrologic data	Discharge data Zambezi River, Katima Mulilo	Department of Water Affairs, Namibia	1965–2009
	Discharge data Kwando River, Kongola	Department of Water Affairs, Namibia	1978–2008
	Monthly stage data ENVISAT Altimeter	European Space Agency	2002–2009
GIS and other ancillary data layers	Digital elevation model (DEM), 10-m resolution	Nationsl Planning Commission GIS Division, Namibia	2008
	Orthophotos Caprivi Strip, Namibia, 1-m resolution	Ministry of Lands, Surveying and Mapping, Namibia	2007
	Hydrologic basins of Southern Africa	Geonetwork, Food and Agriculture Organization (FAO)	2009
Field data	Training samples (CIPEC standard protocol)	2007 and Namibia; over 100 water/inundation training samples	2007, 2009

resampling. The MOD13Q1A product is a composite of eight layers including NDVI, EVI, and reflectance in the red, near-infrared, and blue wavelengths.

Multispectral and multitemporal Landsat ETM+ data

To test the accuracy of the flooding extent index calculated based on AVHRR and MODIS imagery, a set of higher-resolution images collected by Landsat 5 and Landsat 7 Thematic Mapper (TM) and Enhanced Thematic Mapper Plus (ETM+) instruments were also acquired for April/May 1986, 1990, 1996, 2002, 2003, 2004, 2007, 2009 and one for August 2001. The nominal spatial resolution of TM and ETM+ is 30 m. We chose the months April and/or May because they represent the beginning of the dry season when vegetation has not reached full senescence yet and are also generally cloud-free months. The data were acquired from a variety of sources, including the USGS Earth Explorer, University of Maryland Global Land Cover

Facility, and the Council for Scientific and Industrial Research, South Africa.

Climatologic data for the region: multivariate ENSO Index, TRMM, and station data

Climatologic and hydrologic data were acquired from relevant Namibian and Botswanan government agencies and from other available sources (Tropical Rainfall Measuring Mission, TRMM) and were used as a secondary means of data validation for the remote sensing analysis. We used the Multivariate ENSO Index for the period 1950–2010 to gain an initial understanding of the dynamics of dry and wet years for the Southern African region in relation to larger-scale sea–land teleconnections. Multivariate ENSO index (MEI) is calculated based on six major variables measures over the Tropical Pacific Ocean: sea level pressure, zonal and meridional components of the surface wind, sea surface temperature, surface air

temperature, and total cloudiness fraction of the sky (Wolter 1987; Wolter and Timlin 1998).

The mean monthly and annual total precipitation data between 1945 and 2008 for several stations, including Kasane meteorological station, in the basin were obtained from the Department of Meteorological Services, Botswana. Secondly, the monthly averages of rainfall calculated from daily rainfall values for the basin were obtained from the TRMM 3B43 for the period between January 1998, when the mission started, and May 2009 (Fig. 3). TRMM data have been used successfully in previous studies and have been shown to perform well for these latitudes, comparing well with measured rainfall stations throughout the region (Huffman et al. 1997; Kummerow et al. 2000; Nicholson et al. 2003).

Hydrologic and stage data: monthly averaged discharge and water-level data on the Zambezi River and ENVISAT Altimeter stage data for the Chobe River at Kasane

The mean, maximum, and minimum monthly discharge data for the Zambezi River at Katima Mulilo and the Kwando River at Kongola between 1965 and 2009 were obtained from the Department of Water Affairs, Namibia, while the same type of hydrologic measurements for the Chobe and Kwando Rivers were obtained for 1978–2008 from the Department of Water Affairs, Botswana. The data for the Kwando were, however, very unreliable and scattered and were therefore impossible to use in the analysis. Finally, the average monthly stage data (water level measured relative to bank elevations) for a representative Chobe reach upstream from the confluence with the Zambezi River were retrieved from the European Space Agency's ENVISAT Radar Altimeter for the period of operation from 2002 to 2009.

Training samples collected throughout CRB during field visits in 2007 and 2009

Training samples were collected using a well-established and standardized training sample protocol customized for semi-arid environments (CIPEC 2005). The field data collection includes data such as geolocation; topography; land use and land cover type; amount of disturbance; presence of wild/domestic animals; vegetation structure estimates (dominant and secondary species, percent canopy closure, percent ground cover, species diameter at breast height, and height); presence of managed species; land use history; multidirectional photographs; and other site-specific information. We used a randomly stratified by distance data collection approach and gathered a total of 129 permanent water and/or seasonally inundated samples from both field visits.

Data analysis methods

We investigated how regional precipitation and discharge are mechanistically related to the spatial extent and timing of flooding and how the connection between the Zambezi, Chobe, and the Kwando River through the Linyanti swamp affects the spatial extent of flooding in the Chobe floodplain. The end objective was the creation of a 30-year time series of inundation in the CRB.

Chobe River Basin delineation

Typical hydrological–GIS tools for delineating drainage areas are not effective in semi-arid regions with low topographic gradients and underlain by porous sandy substrates. Moreover, the lack of an accepted hydrologic definition for the Chobe Basin and the poor understanding of the region's surficial hydrology complicated the process of basin delineation. We digitized the drainage area of the Chobe–Linyanti system, as well as the Mamili and Zambezi Wetlands, on screen with visual analysis and based on a 10-m spatial resolution DEM, 1-m spatial resolution orthophotographs for 2007, a set of AVHRR NDVI and MODIS EVI images for various months of the year, permanent water training samples collected in 2007 and 2009, and various other hydrologic geospatial datasets for the larger Zambezi watershed. Other ancillary datasets such as NASA/GSFC MODIS Rapid Response images for the 2004 floods and UNOSAT imagery provided by the Department of Water Affairs in Namibia for the 2009 floods in the Zambezi Basin were also used for reference in the drainage delineation process. The delineation process mainly consisted of using the above data and manually digitizing the watershed divide for each of the three subsystems included into CRB. To better understand the surficial hydrology and connectivity within Chobe watershed and better quantify the change in flooding extent

through time, we included the Zambezi West wetland (hereafter referred to as Zambezi wetland) and the Mamili wetland, directly fed by the Zambezi and Kwando Rivers, respectively, in the Caprivi Strip of Namibia.

Identification of flooding extents from Landsat ETM+ data and ground data

We used two main methods for deriving inundation extents from Landsat imagery: (a) supervised classifications using training sample data and (b) a normalized difference water index (NDWI) (Rogers and Kearny 2004). First, the Landsat scenes used for this analysis underwent a set of standard pre-processing operations, including atmospheric calibration, geometric correction and re-projection, and image mosaicking as the study area extends over more than one single path and row.

(a) We created a series of supervised classifications to extract the water extent for CRB. The accuracy testing was performed with ground data collected in May–July 2007 and May–August 2009 (129 water training samples total). The overall classification accuracy was higher for the April 2009 mosaic (93 %, with a kappa value of 0.88) because we had more training samples (or ground control points) than for the May 2007 mosaic (89 %, with a kappa value of 0.84). Signatures from the 2009 classification were then applied back in time to all the other dates, except for 2007. The spatial extent of inundation thus obtained from the supervised classifications on Landsat data was then compared to the corresponding dates/months of the AVHRR/ MODIS-derived inundation (see "Delineation of flooding extents in CRB from coarse- and moderate-resolution satellite imagery"), and a per image regression coefficient was calculated for each image pair by subsetting the AVHRR/MODIS data to match the Landsat data resolution (Table 2).

(b) Secondly, we calculated an NDWI for each Landsat image: $[(\mathrm{RED}-\mathrm{SWIR})/(\mathrm{RED}+\mathrm{SWIR})]$, where RED is the surface reflectance value (0.63–0.69 μm, ETM+ Band 3) and SWIR is the short-wave infrared band (1.55–1.75 μm, ETM+ Band 5). Water pixels were reclassified where NDWI was ≥0.8 (Rogers and Kearny 2004; Sakamoto et al. 2007). We used the NDWI

Table 2 Estimated accuracy of the flooding extent calculated from AVHRR and MODIS data relative to the flooding extent derived from Landsat images for the Chobe River Basin

Year of acquisition	Landsat 174_72	AVHRR/MODIS (DOY)	R^2
1990	04/16	April MVC	0.70
1996	05/02	May MVC	0.68
2001	08/28	241	0.93
2002	04/09	97	0.95
2003	04/28	113	0.82
2004	05/16	129	0.90
2007	05/01	129	0.94
2009	05/06	129	0.96
2009	05/22	145	0.87

to compare to the supervised classifications, and the agreement was generally high, except for the 2001 image which was an August image instead of April/May images.

Delineation of flooding extents in CRB from coarse- and moderate-resolution satellite imagery

Given that the only dataset available for our region as far back as 1985 was an AVHRR NDVI dataset, we used the NDVI product to obtain the spatial extent of the flooding for that time period. For the period 2000–2010, we used both the NDVI and EVI products and concluded that the EVI product performed much better by comparison and when tested against higher-resolution imagery.

For the AVHRR and MODIS NDVI data, we used image-specific thresholds to determine the extent of flooding relative to the larger known water body in the image, namely, Lake Kariba, and ground-referenced water pixels along a stretch of the Chobe River before its confluence with the Zambezi at Kasane similar to the approach by Birkett (2000) and All (2006) (Fig. 4). The threshold differed from image to image as a function of the season and extent of inundation in each image, but because the approach of selecting the histogram-based midpoint between water and land as the upper limit for thresholding the image could not remain consistent for the entire time series analysis of NDVI data from 1985 to 2010, we used this as a baseline and complemented the analysis with a series of ten-class maximum likelihood unsupervised
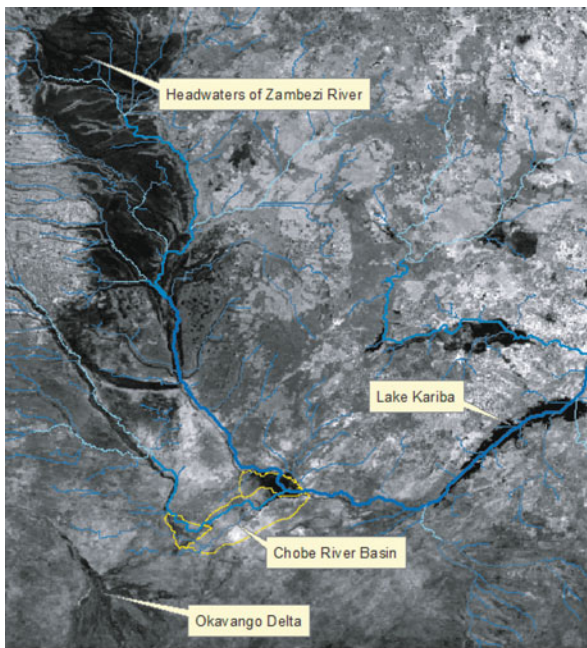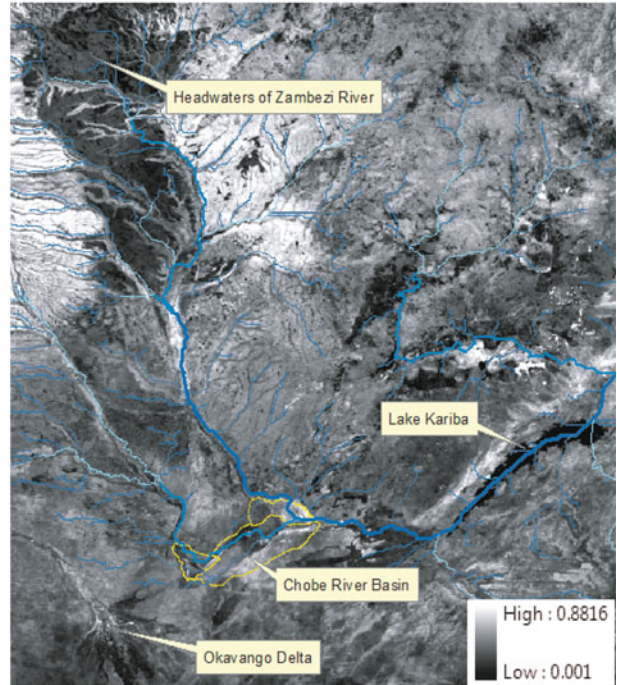
MODIS EVI Image for March 21 (DOY 081),2008
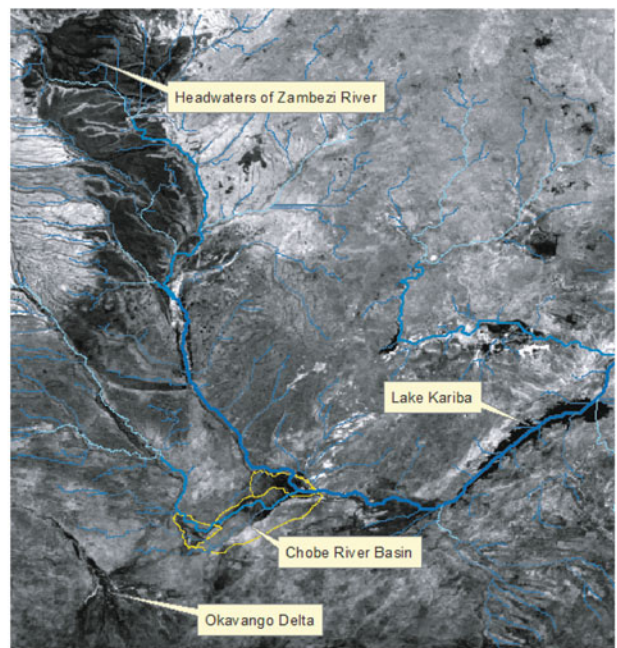
MODIS EVI Image for April 22 (DOY 113), 2008
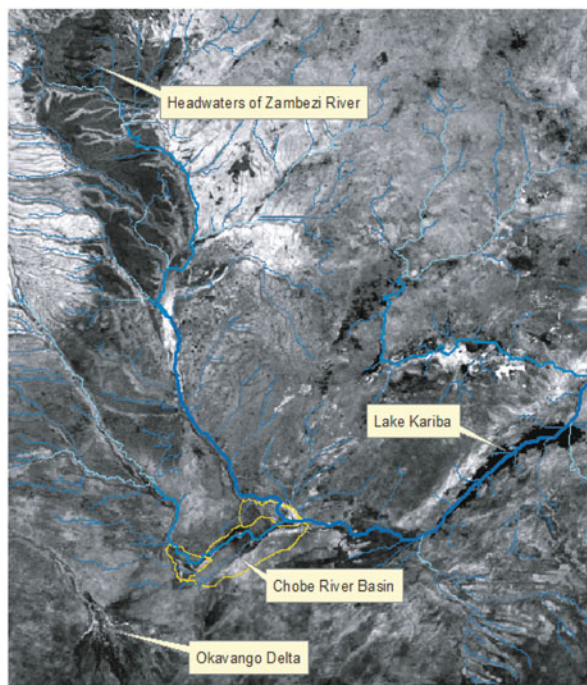
MODIS EVI Image for May 24 (DOY 145), 2008

MODIS EVI Image for June 25 (DOY 177), 2008

Fig. 4 Series of MODIS EVI images from March to June 2008 showing the progressive movement of water from the headwaters of Zambezi through CRB. Note that Lake Kariba to the northeast of CRB was used as a reference for determining the accuracy of flooding extent delineation in the CRB in a first phase of the analysis. *Lighter tones* indicate healthy, photosythetically active vegetation, while *darker tones* indicate no vegetation (including water). *Thicker blue lines* for the stream network indicate higher stream order, the main trunk of Zambezi being stream order 5

classifications performed on the AVHRR and MODIS data (McCarthy et al. 2003). In order to reduce the number of classes that resulted from the unsurpervised classification, we obtained water classes from supervised maximum likelihood classifications of the Landsat images. We used the validated water classes to match against the water extent obtained from unsupervised classifications of both the AVHRR and MODIS NDVI data to determine the appropriate number of classes from the unsupervised classification that should be retained. We selected two classes: one of pure water and one of mixed pixels. Once the number of classes that represent water in the unsupervised AVHRR and MODIS classifications have been determined using the validated Landsat supervised classifications, the total inundation extent for each image date was computed for each of the image subsets. The total inundation extent was calculated by adding the total number of pixels and multiplying them by the sensor's pixel area (0.0625 km^2 for MODIS and 1.1 km^2 for AVHRR).

Furthermore, because the flooding extent analysis using only NDVI for the MODIS images compared relatively poorly with the validation Landsat images, we decided to run a subsequent analysis of annual inundation extent using the MODIS EVI data (Sakamoto et al. 2007, 2009). Each 16-day EVI image was individually reclassified using a baseline threshold of ≤0.2 (pure water pixels) and ≤0.3 (mixed pixels) which represent the lower boundary condition of vegetation (Huete et al. 1999). These EVI values are primarily associated with water bodies and snow/ice, and the basic premise is that the lower baseline contains only non-photosynthetic targets (Sakamoto et al. 2007; Mildrexler et al. 2009; Yan et al. 2010). If the EVI value was ≤0.2, the water-related pixels were defined as flooded pixels, and if $0.2 \geq$ EVI≤0.3, they were reclassified as mixed pixels. If EVI was >0.3, the pixel was reclassified as non-flooded. This was performed on an individual image basis. Next, we created maps of the intra-annual inundation distribution to capture the progressive movement of the flood pulse through the landscape (Fig. 5).

Analysis of remotely sensed-derived time series of flooding extent relative to our specific objectives

- Determine the intra-annual distribution of the flood pulse in the CRB relative to runoff in the Zambezi and Kwando Rivers and regional precipitation

To understand the relative contributions of flood waters spreading into the Chobe–Linyanti floodplain from the Zambezi vs. the Kwando Rivers at different times of the year, we subset the flooding extent maps into three individual sub-basins: the Zambezi Wetlands, Chobe–Linyanti, and Mamili wetland. We calculated the area flooded through time in each of the three sub-basins and the percentage of the total area flooded for every month. We then correlated the area flooded in every sub-basin with the average monthly discharge for individual years in the Zambezi and Kwando, respectively, and with the mean monthly regional precipitation values to account for the relative importance of these sources to flooding.

- Determine the inter-annual distribution of the flood pulse in the CRB

To determine the change in spatial extent of the flooding through time and compute an annual flooding extent index, the images for all the years were recoded into binary values (1=water and 0=non-water), without inclusion of the mixed pixel classes for either AVHRR or MODIS data. We aggregated both the AVHRR 10-day data to a monthly MVC and the MODIS 16-day data to a single-value MVC (approximately representing a monthly composite based on Julian dates). The monthly scenes for individual years were added together, so areas that are flooded throughout the year received a score of 12 and areas that are flooded only partially throughout the year will receive a score that indicates the number of months each pixel was flooded.

- Create a longitudinal (time series) analysis of changes in the spatial extent of flooding in the CRB

Finally, to test the hypothesis that, as indicated by key informant interviews in the region and suggested by other regional findings, the annual flooding extent in CRB has decreased through time, we plotted the AVHRR and MODIS EVI data through time on a monthly and yearly basis and calculated a linear trend and a departure from the median value for both data series. We also calculated a linear trend in total annual precipitation for the Kasane and Katima Mulilo meteorological stations and TRMM data, as well as a similar trend in the Zambezi discharge data.

Fig. 5 Remote sensing workflow showing the pre-processing and processing steps performed to obtain the extent of flooding time series for CRB. *Colored boxes* show the three different imagery datasets used in the analysis, and *arrows* indicate the order in which operations were performed
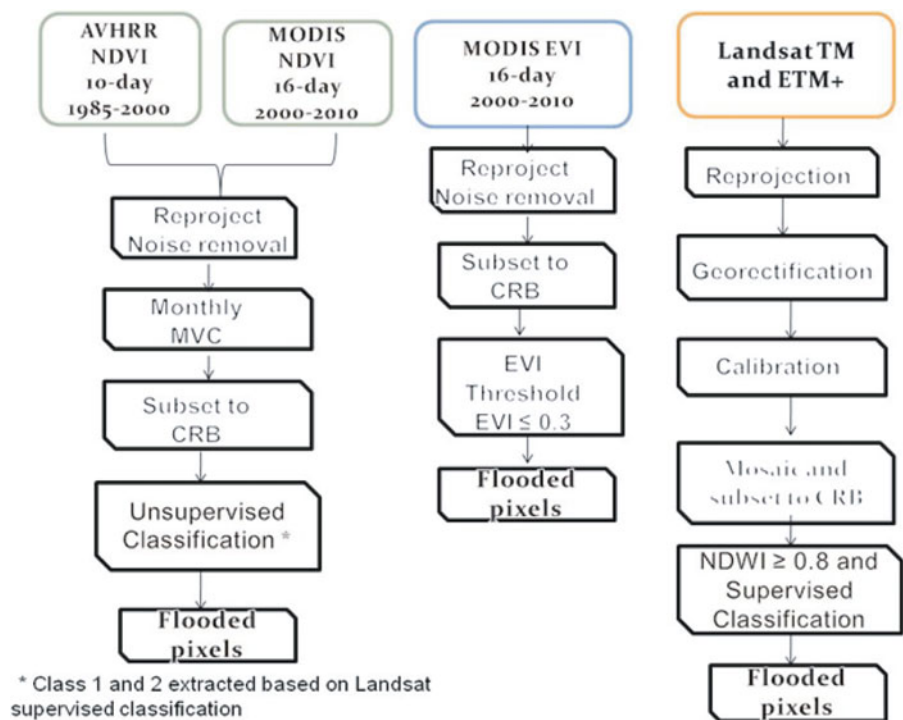

Results and discussion

Intra-annual timing and spatial distribution of the flood pulse in the Chobe River Basin

Our assessment of the magnitude and timing of the flood pulse in the Chobe River Basin is the first such attempt to understanding the surface water connections in this semi-arid watershed. It was previously held that most of the water in the Chobe and its floodplains arrives by backflow from the main trunk of the Zambezi River, near Kasane in Botswana (Susan Ringrose, Okavango Research Institute, 2009, personal communication). However, our analysis shows that the primary and largest flood pulse arrives as the discharge in the Zambezi reaches its peak, at the end of March–April (Fig. 6), and subsequently slowly spreads across the Zambezi wetlands in the Caprivi Strip of Namibia first (Fig. 7). The intra-annual flow distribution of the Zambezi is typical of this climate region with distinct wet and dry seasons, a unimodal peak, and correlates well with stage data recorded by the ENVISAT Altimeter (2009) (r=0.91). This is the first instance when station-measured discharge data were plotted against altimeter-derived stage data for this river system and is an important cross-check of both

data types. They both in turn correlate well with our satellite-derived spatial extents of flooding in the basin (Figs. 7 and 8). We chose 2008 because it was the most complete stage record retrieved from ENVISAT.

Because the hydrologic year for this region actually begins at the beginning of the wet season, in November, water throughout the basin is relatively dispersed spatially and generally concentrated in the Lake Liambezi region or shallow depressions in the landscape as a result of local and regional precipitation primarily (Fig. 7). As Fig. 7 shows, the number of pixels reclassified as mixed ($0.2 \geq EVI \leq 0.3$) is highest during the period from November to February before the flood pulse from the Zambezi starts moving through the system and a larger volume of water spreads on the landscape. As discharge peaks in the Zambezi starting in mid-March and April, water spreads out across the Zambezi wetlands first and is also being pushed as backflow into the main Chobe channel, so by the end of March (DOY 081), the flood pulse enters the floodplains of the Chobe (Fig. 7). The maximum extent of flooding in CRB occurs in April and May, and as the water recedes from the Zambezi wetlands and the northeastern part of the basin, it begins to concentrate in Lake Liambezi and the surrounding lower floodplain of the Chobe–Linyanti.

Fig. 6 Intra-annual Chobe stage–Zambezi discharge relationship for 2008; Chobe stage data upstream from Kasane from the ENVISAT Altimeter and Zambezi mean monthly discharge at Katima Mulilo Station from the Department of Water Affairs, Namibia. The Pearson correlation coefficient (r) is 0.91
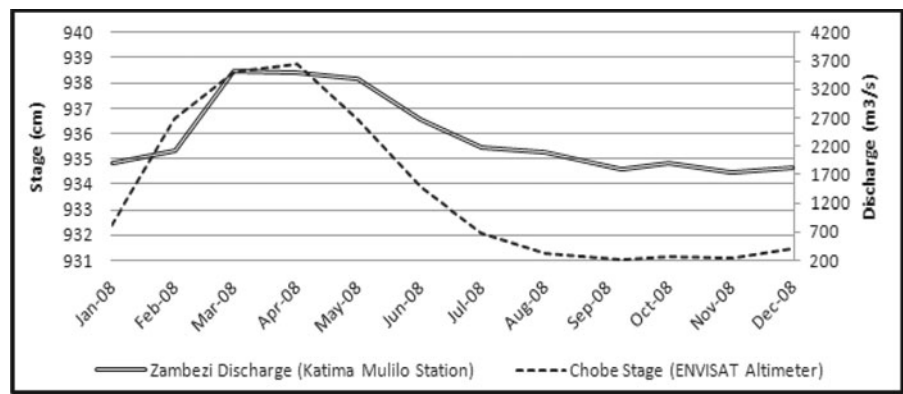
By the middle of the dry season and depending on the hydro-climatological nature of the year, CRB receives water through sporadic connections from the Linyanti channel, which are directly fed by flood waters from the Kwando River making their way into Mamili wetlands. This secondary, smaller, dry season flood pulse is due to the different flow regime of the Kwando River whose discharge peaks in June–August, as opposed to March–April, as is the case for the Zambezi River (Fig. 6). The intra-annual flood pulse distribution in CRB described in Fig. 7 for 2009 is representative in terms of the progressive spatial distribution of the flood pulse, with variations in extent captured in Fig. 9 for the entire time series analyzed from both AVHRR NDVI and MODIS EVI data. We chose the 2009 data to show the intra-annual distribution of flooding because we had very recent station and altimeter-derived data as well as ground data (training samples) to validate the flooding extent areas. The year 2009 also happened to be one of most noise-free annual time series derived from the MODIS EVI data.

Figure 8 shows a breakdown of CRB into the three hydrologically different constituent sub-basins and the typical timing of the flood pulse moving through the system. Similar to Fig. 7, Fig. 8a shows the flooding extent at its greatest in the Zambezi wetlands from the beginning of March to May; commonly, between 45 and 60 % of the Zambezi wetlands area is flooded, the extent being the highest during the 2009 and 2010 high years of flooding (almost 70 % of the total sub-basin area; Fig. 8b). Within <2 weeks, the flood pulse makes its way into the Chobe, in the low floodplains of the communal lands in Botswana and also into Lake Liambezi (Fig. 8a).

Throughout the year in the Chobe, the extent of flooding decreases after the Zambezi water pulse recedes and then increases once more, although not as dramatically and depending on the discharge by the Kwando, toward the end of June–July when the flood pulse from the Kwando arrives in Mamili (Fig. 8a). The mean of the total area of the Chobe flooded on an annual basis ranges from about 5 % to almost 20 % during the peak extent of flooding for years with higher flooding, such as 1989, 1991, 2009, and 2010.

In the Mamili wetland, the flood pulse from the Kwando River arrives as the discharge peaks at the hydrologic station upstream of the wetland (specifically at Kongola, Namibia) toward the end of June and July (Fig. 8a). During the year, typically, the lowest extent of flooding occurs between March and June and at the end of the dry season, and because most of this area lies in a depression created by the extensive fault system underlying the region (Gumbricht et al. 2001), water also tends to accumulate on the surface with the onset of the rainy period, covering between 20 and 40 % of the area (Fig. 8b).

Finally, to understand the mechanistic relationship between discharge in the Zambezi, which accounts for most of the flood pulse to the Chobe, and areas inundated on an annual basis, we ran correlations between the mean monthly discharge calculated from daily data and total area flooded on a monthly basis. The proportion of area of the Zambezi wetlands inundated on an annual basis correlates strongly with discharge in the Zambezi ($0.89 \geq r \leq 0.93$, correlation significant at the 95 % confidence interval) for most of the years in the time series of both AVHRR and MODIS data. However, the variation in discharge in the Zambezi only accounts for between 32 and 39 % of variation in the annual extent of flooding in the main Chobe basin ($0.32 \geq r \leq 0.39$, significant correlation at the 95 % confidence interval). This is probably explained, on the
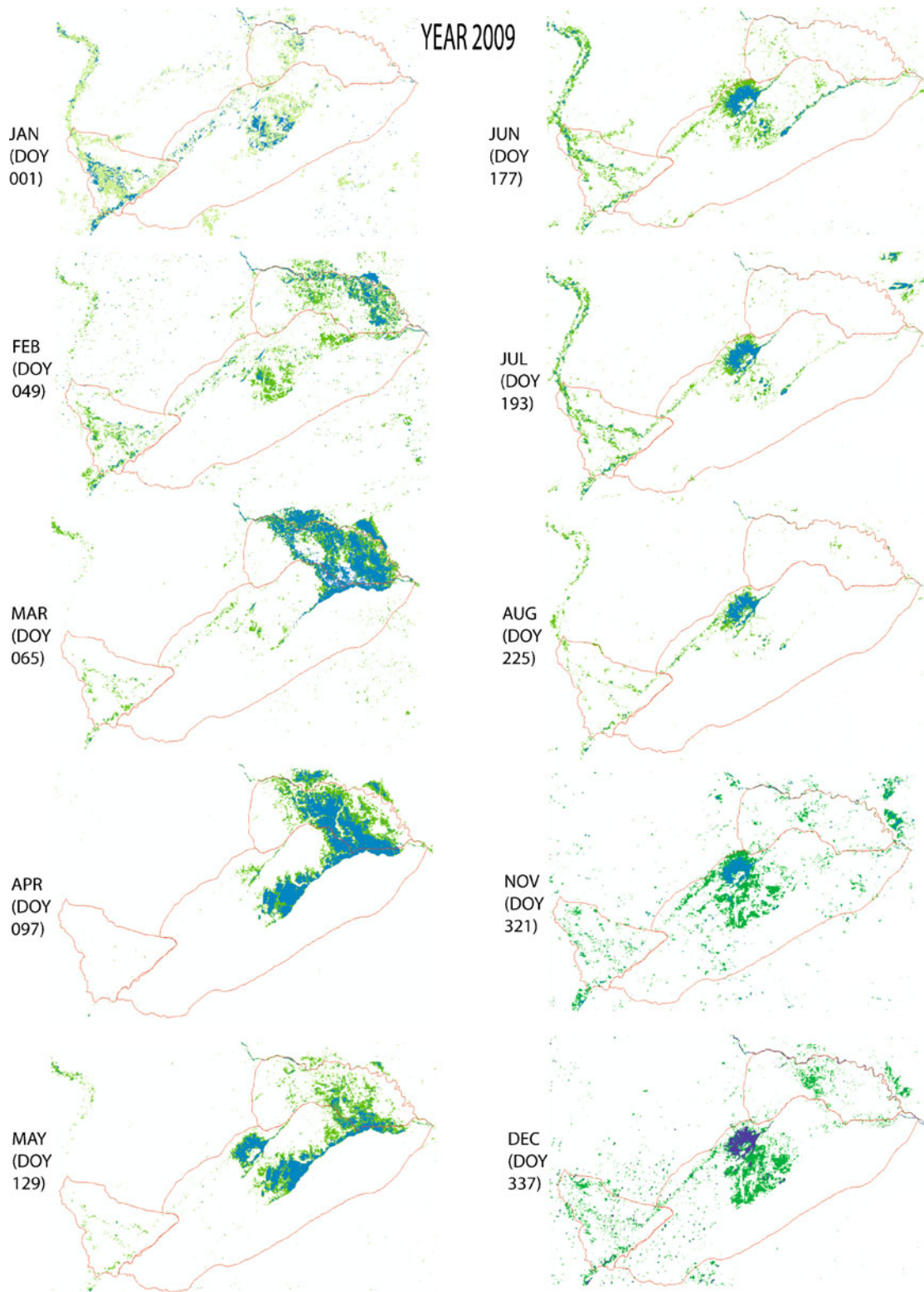
Fig. 7 Spatial distribution of inundation in the Chobe–Zambezi–Mamili system during 2009, with September and October missing due to low spatial extent of flooding. *Blue areas* indicate the distribution of flooded pixels, while *green areas* indicate mixed pixels
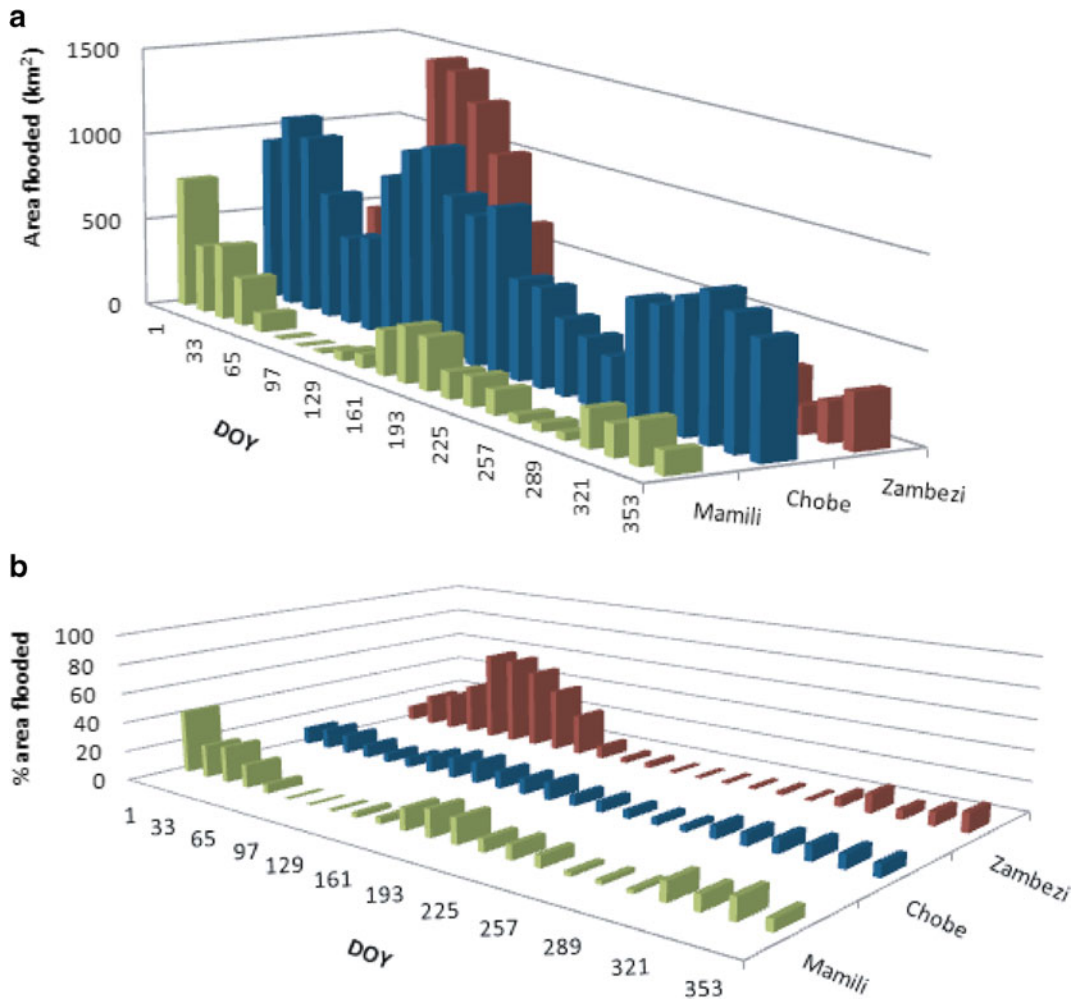
Fig. 8 **a** Timing of the flood pulse in the three individual sub-basins of Chobe River Basin, Mamili, Zambezi, and Chobe–Linyanti Floodplain, shown in Julian days for 2009 as a function of the 16-day flooded area. **b** Graph showing the percentage area flooded of the total area (0–100 %) for the three sub-basins of CRB in Julian days for 2009

one hand, by the 2-week to 1-month lag between peak discharge in the Zambezi and the highest extent of flooding in the Chobe. On the other hand, variations in surficial flow connections with Mamili, the amount of water accumulated in Lake Liambezi, and the length of time before evaporation also contribute to explaining this fairly low correlation. Finally, the contributions of water from regional precipitation during the rainy season might also be a contributing factor in explaining why the amount and timing of discharge in the main Zambezi trunk and the extent of inundation in the Chobe are less linked than previously expected. The correlation between the area flooded and local precipitation as recorded at the meteorological station

closest to the confluence between the Chobe and Zambezi (Kasane, Botswana), as well as TRMM data, is not significant at the 95 % confidence interval and only accounts for <10 % of the areal flooding extent variability throughout the year.

Inter-annual changes in the flooding extent
in the Chobe River Basin

Figure 9 below shows the inter-annual spatial extent of flooding as calculated from the 16-day MODIS EVI data, showing only the years from 2001 to 2009 and only the pure water class (the mixed pixel class was not included in these maps as we could not validate
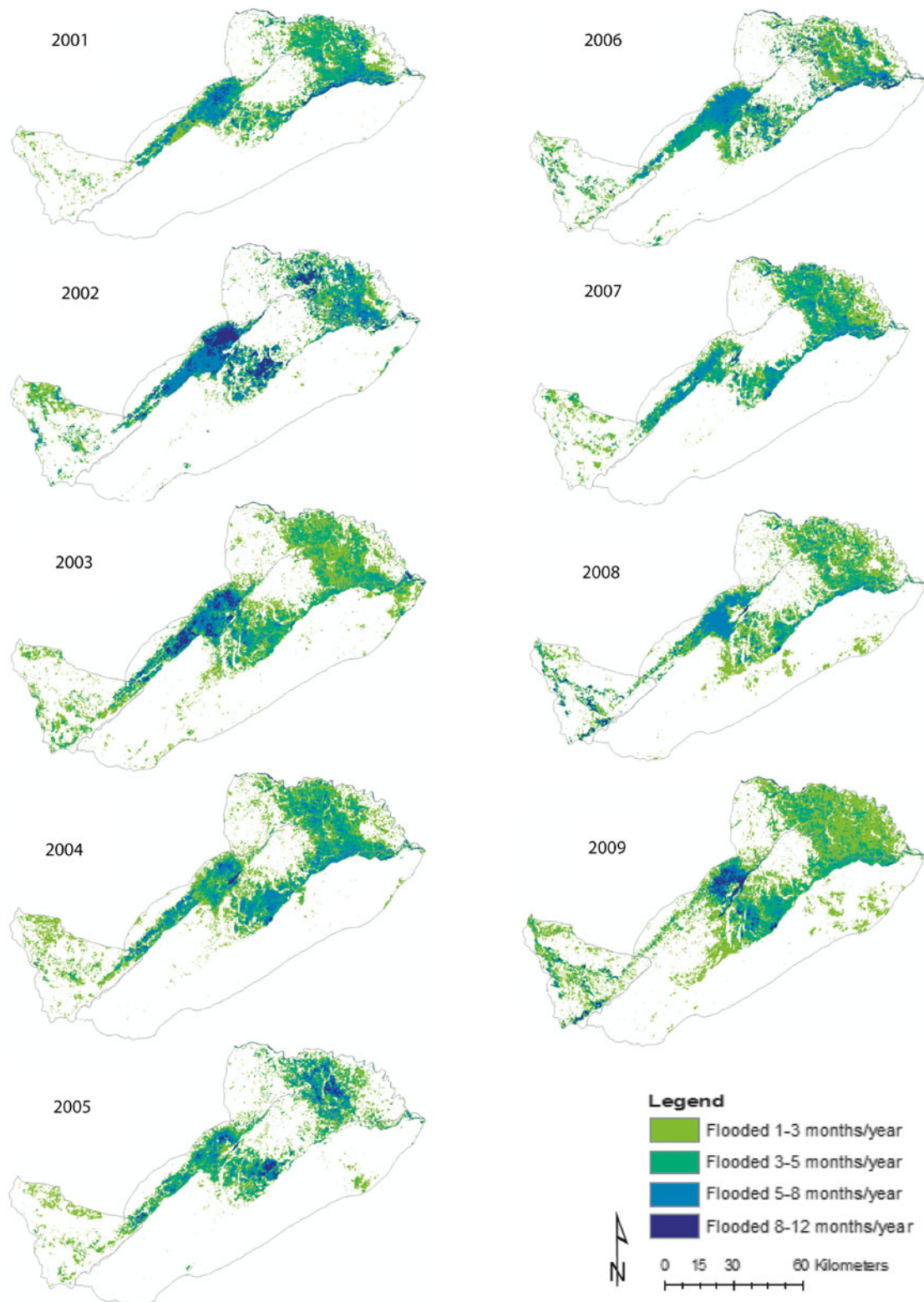
Fig. 9 Spatial extent of flooding (flooding extent index) calculated for individual years for the Chobe River Basin from MODIS EVI data for the period 2001–2009

that on the ground and tried to avoid overestimation of the flooding extent). We did not show 2000 or 2010 because we do not have the complete data series for those years and the resulting scores for inundation are on a different scale than the other years we have a complete data record for.

Surface water is present in the CRB for more than 8 months of the year only along the main channel of the Chobe and parts of Lake Liambezi, depending on the nature of the hydro-climatological year. Most of the surface area inundated annually is usually inundated for <3 months per year, especially in the Zambezi wetlands where the depth of inundation can reach up to 2–4 m during flooding events, but is generally not very high. There are depressions in the landscape (locally known as milapo and covered by aquatic grasses when flooded) where water remains at the surface for 3–5 months of the year, especially along the main Chobe floodplain, areas of the Mamili wetland, and parts of the Zambezi wetlands in eastern Namibia. The communities living in these areas are small and usually located on islands in the landscape due to the very nature of the inundation dynamics through the year in that region. Much of the water detected in Mamili during the wettest months of the year (December to February; see Fig. 8a) is mostly in the mixed pixel category as the water tends to be covered with vegetation (personal observation) and because the discharge remains fairly constant through the year; hence, the spatial extent of flooding in Mamili tends to be underestimated when including only the pure water pixels.

Figure 9 shows the lowest spatial extent of flooding which occurred in 2005, followed by 2001 and 2002. Even though the flooding in 2010 and 2011 has been more extensive than the 2009 high flood event, for the data shown, 2009 is the year with the most extensive flooding overall. This figure also shows how dependent the entire Chobe system is on the magnitude of the flood pulse from the Zambezi and how negatively affected the entire ecosystem would be if diversions or other water abstraction schemes were to be implemented upstream along the Zambezi River.

The change in the spatial extent of flooding annually for the period from 2000 to 2010 is closely related to the general flow conditions in the Zambezi River, which accounts for the highest amount of contribution, and the latter correlating fairly strongly with stage data obtained from ENVISAT (Figs. 10 and 11). For the period of interest for this study (1985–2009), the driest year in the

Zambezi in terms of discharge was 1996, while the greatest floods were recorded in 1989, 2001, 2004, 2008, and 2009. For the 1975–2006 period for example, all five major floods (>6,000 m^3/s) were recorded before 1980, while all five lowest discharges (<1,500 m^3/s) were recorded after 1990 (Fig. 10). The overall trend in river discharge for the Zambezi indicates a 7 % average reduction in runoff prior to the 2008–2009–2010 floods, associated with the general trend in decreasing precipitations in Southern Africa since the 1970s (Wessels et al. 2004; Gaughan and Waylen 2012).

Runoff in the Zambezi in turn depends on the overall precipitation trends for the region and the nature and strength of El Niño and La Niña conditions affecting Southern Africa (Fig. 12). For example, the relatively low spatial extent of flooding in 2001 is related in part to the relatively low total annual precipitation rates for that year, although the discharge of the Zambezi was above average and the MEI identifies a negative standardized departure from the long-term average, which makes it a relatively wet year by comparison. During the late 1980s, rainfall was below the 50-year average, while oscillations between wet and dry years starting with the early 1990s have become more extreme under the influence of stronger El Niño or La Niña years (Wessels et al. 2004). Furthermore, work by Gaughan and Waylen (2012) in the region indicates decreasing precipitation patterns and increased dry years and warm phases of ENSO in the last quarter of the twentieth century. For Southern Africa, 1991–1992, 1994–1995, and 1997–1998 have been the driest El Niño seasons, while 1999–2000 and 1995–1996 were the wettest seasons, with the 2001 and 2004 growth seasons being the driest (Fig. 12). Figure 12 shows the period from 1990 to 1995 to be on average 1–2 standard deviations positive departure away from the mean and a similar, but less pronounced, pattern for the period between 2002 and 2006, while the years 2008 and 2009 stand out as higher-than-average wet, with a negative anomaly from the mean conditions included in the MEI. These years also exhibit some of the highest spatial extent of flooding.

Longitudinal (time series) analysis of the spatial extent of flooding in the CRB based on AVHRR and MODIS data: 1985 to 2010

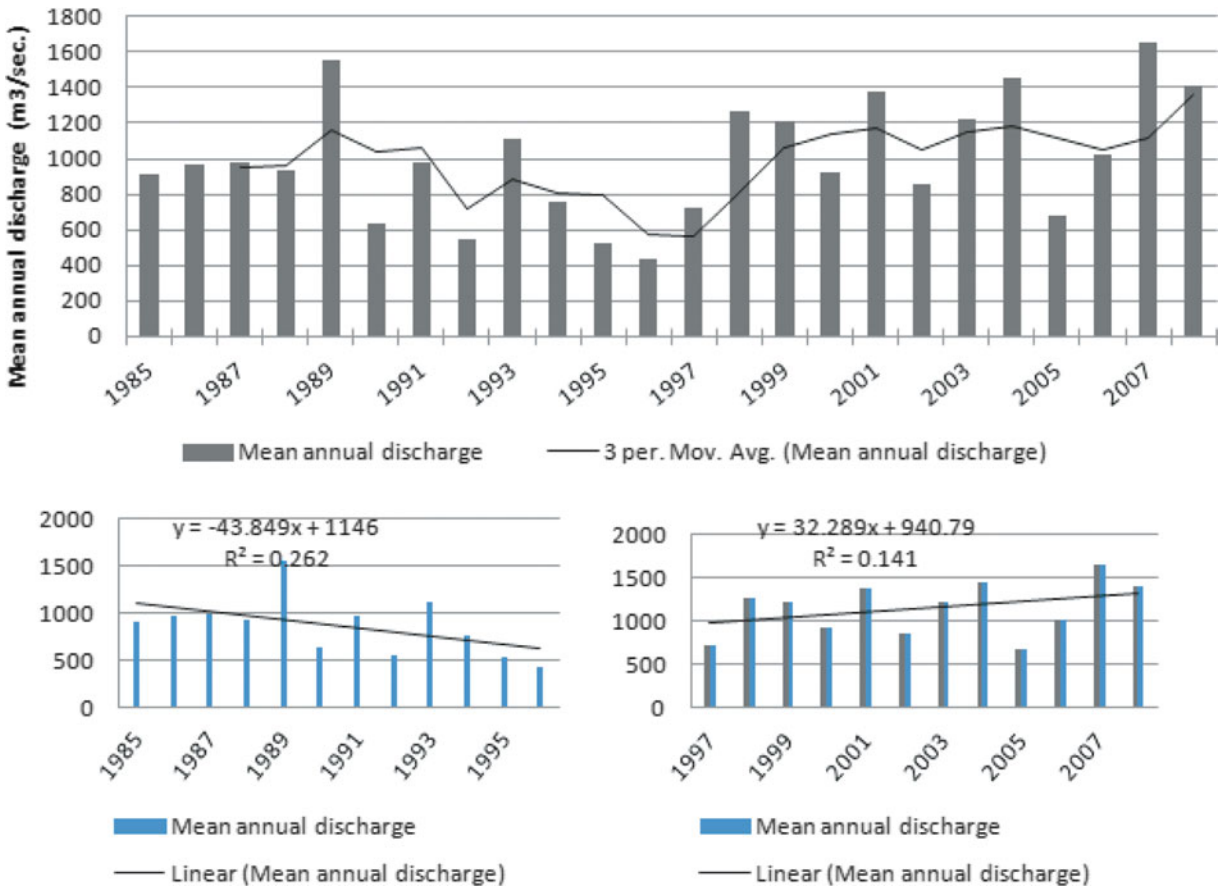To test our hypothesis of whether there has been an overall decreasing trend in the spatial extent of

Fig. 10 Mean annual discharge of the Zambezi River at Katima Mulilo for the period 1985–2009 calculated from total daily discharge. The 3-year moving average for the entire time series shows a decrease for 1985–1996 and a slight linear increasing trend in discharge for the period 1997–2009

Fig. 11 Average monthly stage data for a Chobe reach 25 km upstream from the confluence with the Zambezi River retrieved from the ENVISAT Altimeter on 5 February 2010
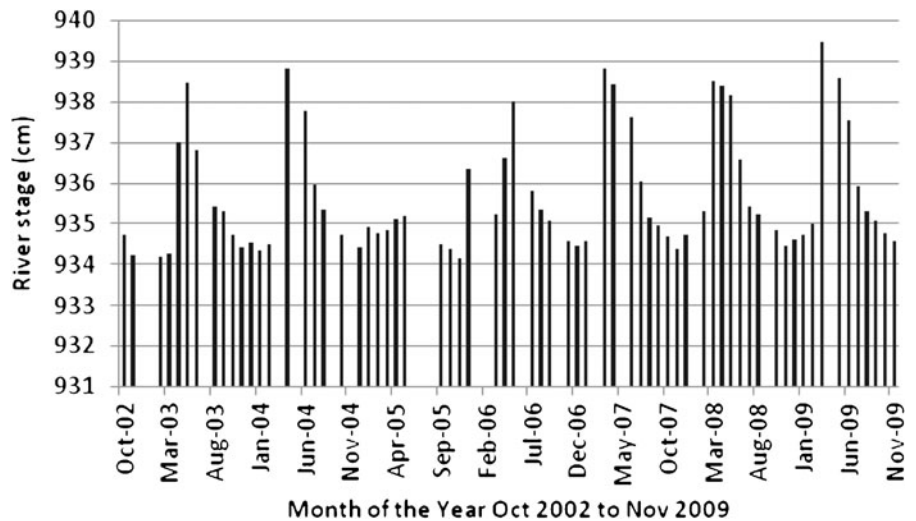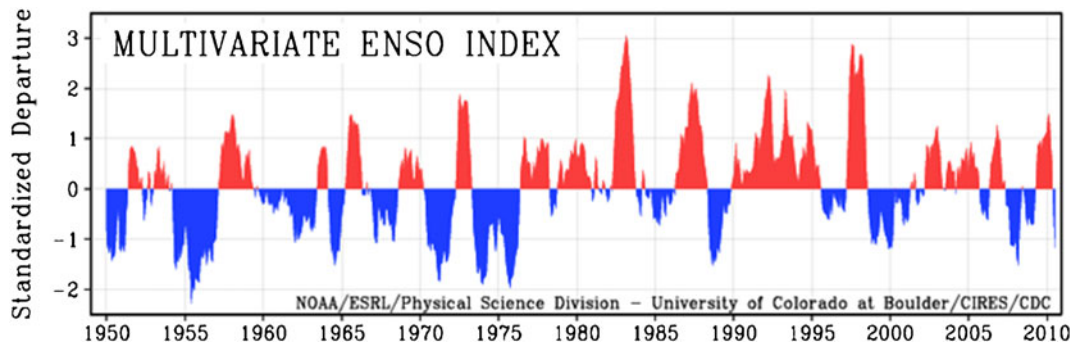
Fig. 12 Total annual precipitation at the Kasane meteorological station in Botswana between 1960 and 2007 and the Multivariate ENSO Index for 1950–2010. Note the correspondence between the dry ENSO conditions between 1990 and 1995 and low annual precipitation values recorded in CRB (precipitation data source: Department of Meteorological Services, Botswana; MEI data source: Wolter and Timlin 1998)

inundation in CRB during the last two and a half decades, we performed a longitudinal time series analysis of the flooding extent data obtained from both AVHRR and MODIS. We performed a simple linear trend analysis as well as a moving average trend analysis and a departure from the median calculation. Because the spatial resolution of the MODIS EVI data is different from the AVHRR ones, the two datasets were best plotted individually to show the trend in flooding extent through time for the CRB system. Overall, the analysis of both the AVHRR and MODIS time series data indicates a consistent decline in the extent of flooding in CRB in the last two and a half decades of the twentieth century by ~4–6 % on average, but this is complicated by the high floods of 2009 and 2010.

The trend analysis of the AVHRR monthly MVC NDVI data reveals a significant decrease in the extent of flooding from 1985 to 2004 for CRB, expressed as area measured at the 1.1-km^2 resolution (Fig. 13). The 1985–2004 median of area flooded on a monthly basis (solid straight line in Fig. 13) is 1,403 km^2 and the mean area flooded is 1,415 km^2. An analysis of the number and magnitude of floods above the median for the period shows a slight dampening of the magnitude of floods through time. The dotted line in Fig. 14 represents the 2-year moving average of monthly flooded area, and while the r^2 for the linear trend through time is <0.10, there is a 4 % decline in flooded area overall.

The trend analysis of the 16-day MODIS EVI data also reveals a decrease in the extent of flooding from 2000 to 2008 for CRB, expressed as area measured at the 250-m spatial resolution. First, we plotted the

period 2000–2008 separately in order to ascertain what the dynamics of flooding were before the major flood events in 2009 and 2010. The linear trend analysis shows a 6.3 % decrease in the area flooded monthly, with an r^2 of 0.15. When we included the 2009 and 2010 data into the analysis, the r^2 for the linear trend through time is <0.10, but overall, there is still a 3.75 % decline in flooded area over the last decade (Fig. 14).

Finally, we aggregated our monthly and 16-day data of the area flooded for the entire CRB into yearly values to determine whether a similar or more consistent trend through time could be observed. While for the AVHRR-based time series the trend in flooded area at a yearly level was not significant (r^2<0.10), for the last decade, we determined a significant decreasing linear trend (r^2=0.32) in flooded area that probably primarily reflects the generally drier than normal climatic anomalies in Southern Africa (Fig. 15), consistent with work by Wessels et al. (2004). The latter finding is slightly confounding, however, as the general trend in runoff in the Zambezi during the last decade for instance is an increasing one (r^2=0.14; see Fig. 10) and may indicate more complex lags and feedbacks in the system, which are beyond the scope of this paper.

Apart from the complexities introduced by the more recent flood events in the basin, interviews with local informants indicate a decrease in the flooding extent of the Chobe River in the last 30 years. Fieldwork in the Chobe basin and research elsewhere in semi-arid flood-dependent ecosystems indicate a strong relationship between changes in flooding extent and changes in the vegetation structure in the floodplain areas
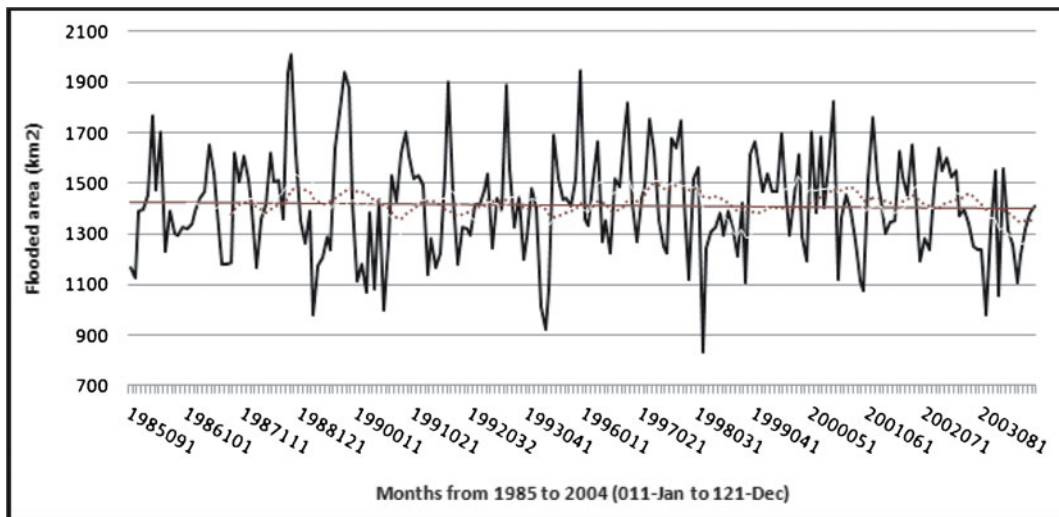
Fig. 13 Flooded area on a monthly basis in CRB from 1985 to 2004 based on an unsupervised maximum likelihood classification of monthly MVC AVHRR NDVI data. The 1985–2004 median (*solid straight line*) is 1,403 km² and the mean is 1,415 km²; the *dotted line* represents the 2-year moving average of monthly flooded area. The R^2 for the linear trend through time is <0.10, but shows a 4 % decline in flooded area

(Westbrooke et al. 2005; Ringrose et al. 2007). Both the literature and local informants suggest that there is a link between increasing rates of bush encroachment in the Chobe floodplains in Botswana and Namibia and the temporal and spatial modifications of the area flooded annually by the river. However, characterizing the relationship between changes in the flooding regime and vegetation patterns is difficult due to the poor understanding of the present and past spatial extent and dynamics of the floods in the basin. Thus, the present analysis represents a contribution in that direction.
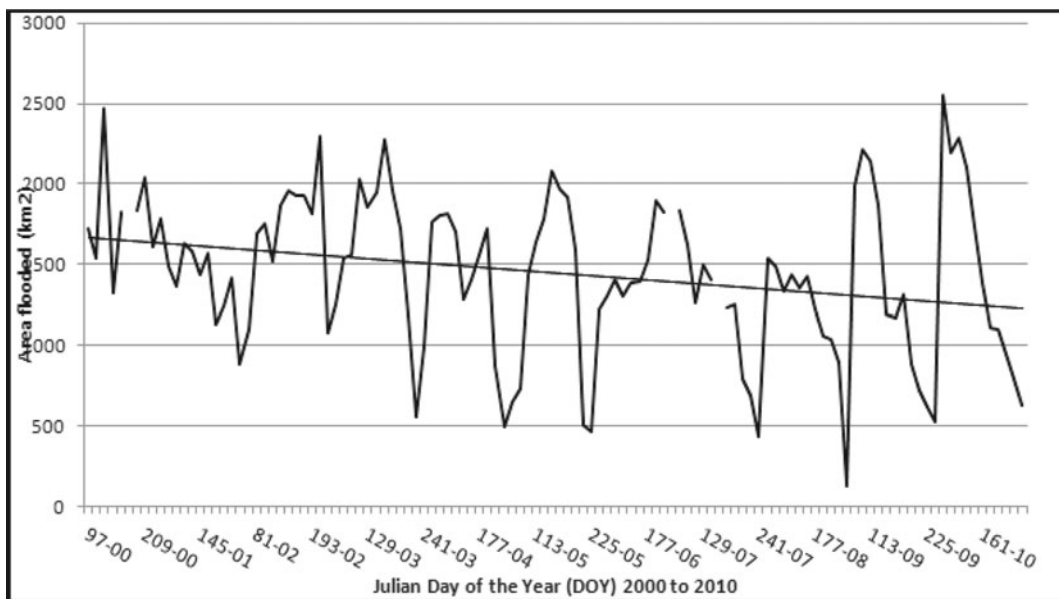

Fig. 14 Flooded area on a monthly basis in CRB from 2000 to 2010 based on thresholding of the 16-day MODIS EVI data. The R^2 for the linear trend through time is <0.10, but shows a 3.75 % decline in flooded area over the last decade, even including the last 2 years of higher flooding

Fig. 15 Flooded area aggregated to yearly values for the entire from total monthly flooded area Chobe River Basin (including the Zambezi and Mamili Wetlands) aggregated for 2000–2010 from MODIS EVI data (includes both pure and mixed water pixels)
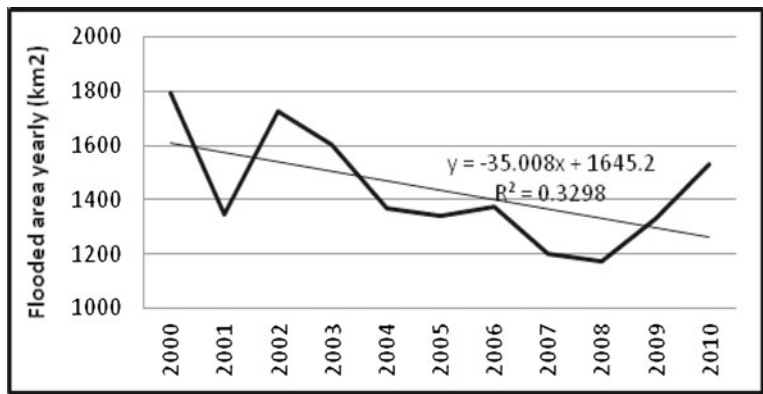
One of the main limitations of this study results from unavoidably underestimating the spatial extent of flooding and possible misclassifications caused by the presence of wildfires which have a similar spectral signature in the visible spectrum bands to water. The underestimation of burned area is primarily due to the data type used in the analysis, namely, vegetation indices, as opposed to potentially more sensitive remotely sensed data, such as thermal imagery which has been shown to better differentiate between surfaces with relatively similar spectral signatures in the visible part of the electromagnetic spectrum, especially the red, blue, and near-infrared bands used in deriving the NDVI and EVI products (Cassidy 2007).

Of importance for water resource management purposes in light of the water abstraction scheme developments planned for the Chobe to start by 2015, as well as for more general natural resource management in the region, is the seasonal and intra-annual distribution of the flooding. By creating maps of the flooding extent index through time for individual years, we determined that the areas most likely to be flooded on a more permanent basis are Lake Liambezi and channels in the Mamili wetland and parts of the Linyanti channel, as well as the main river channel and low-lying floodplains of the Chobe where waters gets pushed into from the Zambezi or across the eastern Caprivi Region (Zambezi wetlands). The main floodplain of the Chobe–Linyanti and areas in the easternmost part of the Caprivi Strip are likely to experience annual flood pulses that last between 5 and 8 months, depending on the amount of regional precipitation and river runoffs in the Zambezi and Kwando Rivers. The areas that are only occasionally flooded during high-intensity precipitation or flooding events include the bottom reaches of the Mamili wetland, the densely populated villages spread in the eastern part of the Caprivi Region in the higher portions of the floodplain, as well as some of the more isolated pans and water depressions in the Chobe National Park on the more elevated part of the Chobe floodplain.

Conclusions

The remotely sensed data and meteorological and hydrological analyses reveal a decreasing trend in the extent of flooding from 1985 to 2009 by approximately 6 % and a 2-week to a 1-month lag between the highest discharges in Zambezi River and the highest extent of flooding in the Chobe Basin, thus quantifying for the first time for this system the interconnections between the Chobe and Zambezi systems. River flow in the Zambezi represents the main source of water for the Chobe Basin both through surficial connections across the Zambezi Wetlands and through back-flooding from the main channel. Despite that, discharge in the Zambezi upstream from its confluence with the Chobe accounts for only about 39 % of the extent in area flooded on an annual basis due primarily to a lag in the movement of the water across the landscape, as well as other factors such as storage in Lake Liambezi and subsequent evaporation, inflows from the Kwando through the Mamili wetland, or regional precipitation. We have also shown how dependent the entire Chobe system is on the magnitude of the flood pulse from the Zambezi. This finding implies that this entire system would change if diversions or other water abstraction schemes were to happen upstream along the Zambezi River. This paper is the first attempt to perform such an analysis for this

particular system. As such, the results of this paper might form a basis for water resource management and ecosystem management in the study area in the future, even though refinements of the present methodology would greatly improve this initial assessment.

The Chobe River Basin is a key water resource for Botswana both currently and more so in the future for both domestic and irrigated agriculture, as well as for the subsistence communities of Eastern Namibia. It is also a crucial water resource for the abundant wildlife populations and charismatic megafauna in the region that act as a major tourist attraction and represent a very important contribution to the gross national product of both countries. The interest in performing this analysis resulted primarily from key informant interviews during several field visits which revealed changes in the extent of flooding and vegetation structure in floodplain areas, visibly expressed in increasing shrub encroachment. Also, relevant literature on Southern Africa and climate change predictions indicate potentially decreasing annual precipitation values and subsequent decreases in river runoffs that might adversely affect both commercial and subsistence agricultural production, as well as other water resource-related activities in the CRB system in the near future. Future work will include creating inundation maps based on thermal imagery and determining the relationship between changes in flooding extent and grassland-to-scrubland conversions in the Chobe floodplain.

References

All, J. D. (2006). Colorado River floods, droughts and shrimp fishing in the Upper Gulf of California, Mexico. *Environmental Management, 37*, 111–125.

All, J. D., & Yool, S. (2004). Indexing endangered species risk in the Colorado River Delta, Mexico using AVHRR NDVI time series data. *Geocarto International, 19*(4), 5–13.

Alsdorf, D. E., & Lettenmeier, D. P. (2003). Tracking fresh water from space. *Science, 301*, 1491–1494.

Appleton, C. C., Ellery, W. N., Byskov, J., & Mogkweetsinyana, S. S. (2008). Epidemic transmission of intestinal schistosomiasis in the seasonal part of the Okavango Delta, Botswana. *Annals of Tropical Medicine and Parasitology, 102*(7), 611–623.

Birkett, C. M. (2000). Synergistic remote sensing of Lake Chad: variability of basin inundation. *Remote Sensing of Environment, 72*, 218–236.

Boko, M., I. Niang, A. Nyong, C. Vogel, A. Githeko, M. Medany, B. Osman-Elasha, R. Tabo and P. Yanda. (2007). Africa: climate change 2007: impacts, adaptation and vulnerability. In M.L. Parry, O.F. Canziani, J.P. Palutikof, P.J. van der Linden and C.E. Hanson (Eds.), *Contribution of Working Group II to the Fourth Assessment Report of the Intergovernmental Panel on Climate Change* (pp. 433–467). Cambridge UK: Cambridge University Press.

Boulain, N., Cappelaere, B., Seguis, L., Gignoux, J., & Peugeout, C. (2006). Hydrologic and land use impacts on vegetation growth at the watershed scale in a semi-arid environment. *Regional Environmental Change, 6*, 147–156.

Brown, M. E., Pinzon, J. E., Didan, K., Morisette, J. T., & Tucker, C. J. (2006). Evaluation of the consistency of long-term NDVI time series derived from AVHHR, SPOT Vegetation, SeaWiFS, MODIS and LandSat ETM+ Sensors. *IEEE Transactions on Geoscience and Remote Sensing, 44*, 1787–1793.

Bryant, R. G. (1999). Application of AVHRR to monitor a climatically sensitive playa: case study, Chott el Djerid, Southern Tunisia. *Earth Surface Processes and Landforms, 24*, 283–302.

Bryant, R. G. (2003). Monitoring hydrological controls on dust emissions: preliminary observations from Etosha Pan, Namibia. *The Geographical Journal, 169*(2), 131–141.

Cassidy, L. (2007). Mapping the area burned in the wetlands of the Okavango panhandle using a hierarchical classification approach. *Wetlands Ecology and Management, 15*, 253–268.

Center for the Study of Institutions, Population and Environmental Change. (2005). CIPEC's methodological contributions. CIPEC, Bloomington, Indiana. Retrieved from http://www.cipec.org/research/methods. Accessed 15 May 2007.

Chipman, J. W., & Lillesand, T. M. (2007). Satellite-based assessment of the dynamics of new lakes in southern Egypt. *International Journal of Remote Sensing, 28*(19), 4365–4379.

Department of Wildlife and National Parks (DWNP) Botswana. (2009). *Aerial survey on wildlife populations of Botswana*. Botswana: DWNP Gaborone.

Domenikiotis, C., Loukas, A., & Dalezios, N. R. (2003). The use of NOAA/AVHRR satellite data for monitoring and assessment of forest fires and floods. *Natural Hazards and Earth System Sciences, 3*, 115–128.

European Space Agency. (2009). ENVISAT Altimeter. Retrieved 4 February 2009 from http://envisat.esa.int/earth/www/object/index.cfm?fobjectid=6995.

Gaughan, A. E., & Waylen, P. R. (2012). Spatial and temporal precipitation variability in the Okavango–

Kwando–Zambezi catchment, Southern Africa. *Journal of Arid Environments, 82*, 19–30.

Gumbricht, T., McCarthy, T. S., & Merry, C. L. (2001). The topography of the Okavango Delta, Botswana, and its tectonic and sedimentological implications. *South African Journal of Geology, 104*, 243–264.

Huete, A. R., Liu, H. Q., Batchily, K., & van Leeuwen, W. J. D. (1999). A comparison of vegetation indices over a global set of TM images for EOS-MODIS. *Remote Sensing of Environment, 59*, 440–451.

Huffman, G. J., Adler, R. F., et al. (1997). The Global Precipitation Climatology Project (GPCP) combined precipitation dataset. *Bulletin of the American Meteorological Society, 78*(1), 5–20.

Jain, S. K., Saraf, A. K., Goswami, A., & Ahmad, T. (2006). Flood inundation mapping using NOAA AVHHR data. *Water Resources Management, 20*, 949–959.

Jia, Z., & Luo, W. (2009). A modified climate diagram displaying net water requirements of wetlands in arid and semi-arid regions. *Agricultural Water Management, 96*, 1339–1343.

Justice, C. O., Vermote, E., Townshend, J. R. G., Defries, R., Roy, D. P., Hall, D. K., et al. (1998). The Moderate Resolution Imaging Spectroradiometer (MODIS): land remote sensing for global change research. *IEEE Transactions on Geoscience and Remote Sensing, 36*(4), 1228–1249.

Kummerow, C., Simpson, J., Thiele, O., et al. (2000). The status of the Tropical Rainfall Measuring Mission (TRMM) after two years in orbit. *Journal of Applied Meteorology, 39*, 1965–1982.

Liu, H. Q., & Huete, A. R. (1995). A feedback based modification of the NDVI to minimize canopy background and atmospheric noise. *IEEE Transactions on Geoscience and Remote Sensing, 33*, 457–465.

McCarthy, J. M., Gumbricht, T., McCarthy, T., Frost, P., Wessels, K., & Seidel, F. (2003). Flooding patterns of the Okavango Wetland in Botswana between 1972 and 2000. *Ambio, 32*(7), 453–457.

Mildrexler, D. J., Zhao, M., & Running, S. W. (2009). Testing a MODIS Global Disturbance Index across North America. *Remote Sensing of Environment, 113*, 2103–2117.

Mosugelo, D., Moe, S. R., Ringrose, S., & Nelleman, C. (2002). Vegetation changes during a 36-year period in northern Chobe National Park, Botswana. *African Journal of Ecology, 40*(3), 232–240.

Nicholson, S. E. (2001). Climatic and environmental change in Africa during the last two centuries. *Climate Research, 17*, 123–144.

Nicholson, S. E., Some, B., & Kone, B. (2000). An analysis of recent rainfall conditions in West Africa, including the rainy seasons of the 1997 El Nino and 1998 La Nina Years. *Journal of Climate, 13*, 2628–2640.

Nicholson, B., Some, J., McCollum, E., Nelkin, D., Klotter, Y., Berte, B. M., et al. (2003). Validation of TRMM and other rainfall estimates with a high-density gauge dataset for West Africa. Part I: Validation of GPCC rainfall product and pre-TRMM satellite and blended products. *Journal of Applied Meteorology, 42*, 1337–1354.

Peters, D. P. C., & Havstad, K. M. (2006). Nonlinear dynamics in arid and semi-arid systems: interactions among drivers and processes across scales. *Journal of Arid Environments, 65*, 196–206.

Prigent, C., Papa, F., Aires, F., Rossow, W. B., & Matthews, E. (2007). Global inundation dynamics inferred from multiple satellite observations, 1993–2000. *Journal of Geophysical Research, 112*, D12107.

Ringrose, S., VanderPost, C., Mathson, W., Wolski, P., Huntsman-Mapila, P., Murray-Hudson, M., et al. (2007). Indicators of desiccation-driven change in the distal Okavango Delta, Botswana. *Journal of Arid Environments, 68*(1), 88–112.

Rogers, A. S., & Kearney, M. S. (2004). Reducing signature variability in unmixing coastal marsh Thematic Mapper scenes using spectral indices. *International Journal of Remote Sensing, 20*, 2317–2335.

Rutina, L. P., Moe, S. R., & Swenson, J. E. (2005). Elephant *Loxodonta africana* driven woodland conversion to shrubland improves dry-season browse availability for impalas *Aepyceros melampus*. *Wildlife Biology, 11*, 207–213.

Sakamoto, T., Van Nguyen, N., Kotera, A., Ohno, H., Ishitsuka, N., & Yokozawa, M. (2007). Detecting temporal changes in the extent of annual flooding within the Cambodia and the Vietnamese Mekong Delta from MODIS time-series imagery. *Remote Sensing of Environment, 109*, 295–313.

Sakamoto, T., Phung, V. C., et al. (2009). Agro-ecological interpretation of rice cropping systems in flood-prone areas using MODIS imagery. *Photogrammetric Engineering and Remote Sensing, 75*(4), 413–424.

Sankaran, M., Hanan, N. P., Scholes, R. J., Ratnam, J., Augustine, D. J., Cade, B. S., et al. (2005). Determinants of woody cover in African savanna. *Nature, 438*(8), 846–849.

Skarpe, C., Aarrestad, P. A., Andreassen, H. P., Dhillion, S. S., Dimakatso, T., du Toit, J. T., et al. (2004). The return of the giants: ecological effects of an increasing elephant population. *Ambio, 33*, 276–282.

Smith, L. P. (1997). Satellite remote sensing of river inundation area, stage, and discharge: a review. *Hydrological Processes, 11*, 1427–1439.

Snyder, K. A., & Tartowski, S. L. (2006). Multi-scale temporal variation in water availability: implications for vegetation dynamics in arid and semi-arid ecosystems. *Journal of Arid Environments, 65*, 219–234.

Teillet, P. M., Staenz, K., & William, D. J. (1997). Effects of spectral, spatial, and radiometric characteristics on remote sensing vegetation indices of forested regions. *Remote Sensing of Environment, 61*(1), 139–149.

Turton, A. R. (1999). Water and state sovereignty: the hydro-political challenge for states in arid regions. *MEWREW Occasional Paper No. 5, Water Issues Study Group*.

Wang, F., & D'Sa, E. (2010). Potential of MODIS EVI in identifying hurricane disturbance to coastal vegetation in the northern Gulf of Mexico. *Remote Sensing, 2*, 1–18.

Wessels, K. J., Prince, S. D., Frost, P. E., & van Zyl, D. (2004). Assessing the effects of human-induced land degradation in the former homelands of northern South Africa with a 1 km AVHRR NDVI time-series. *Remote Sensing of Environment, 91*, 47–67.

Westbrooke, M. E., & Florentine, S. K. (2005). Rainfall-driven episodic flood events: are they a major factor in moulding New South Wales arid land vegetation patterns? *Australian Geographer, 36*(2), 171–181.

Westbrooke, M. E., Florentine, S. K., & Milberg, P. (2005). Arid land vegetation dynamics after a rare flooding event:

influence of fire and grazing. *Journal of Arid Environments, 61*(2), 249–260.

Wolter, K. (1987). The Southern Oscillation in surface circulation and climate over the tropical Atlantic, Eastern Pacific, and Indian Oceans as captured by cluster analysis. *J Climate Appl Meteor, 26*, 540–558.

Wolter, K., & Timlin, M. S. (1998). Measuring the strength of ENSO events—how does 1997/98 rank? *Weather, 53*, 315–324.

Yan, Y. E., Ouyang, Z. T., Guo, H. Q., Jin, S. S., & Zhao, B. (2010). Detecting the spatio-temporal changes of tidal flood in estuarine wetlands by using MODIS time series data. *Journal of Hydrology, 384*, 156–163.